[redacted]

MARTIN MARIETTA ENERGY SYSTEMS LIBRARIES
3 4456 0360656 9

CENTRAL RESEARCH LIBRARY
DOCUMENT COLLECTION

AEC RESEARCH AND DEVELOPMENT REPORT

ORNL 1671
Effects of Atomic Weapons

DECLASSIFIED
CLASSIFICATION CHANGE
BY AUTHORITY E. J. Murphy 1/31/62
BY: S. Beidel 6/21/62

LABORATORY RECORDS 1954

# NEUTRON FLUX AND TISSUE DOSE STUDIES WITH FISSION THRESHOLD DETECTORS

G. S. Hurst
J. A. Harter
P. N. Hensley
W. A. Mills
R. H. Ritchie

CENTRAL RESEARCH LIBRARY
DOCUMENT COLLECTION

LIBRARY LOAN COPY

DO NOT TRANSFER TO ANOTHER PERSON

If you wish someone else to see this document, send in name with document and the library will arrange a loan.

OAK RIDGE NATIONAL LABORATORY
OPERATED BY
CARBIDE AND CARBON CHEMICALS COMPANY
A DIVISION OF UNION CARBIDE AND CARBON CORPORATION

UCC

POST OFFICE BOX P
OAK RIDGE, TENNESSEE

[redacted]

[redacted]

[redacted]

ORNL-1671

This document consists of 25 pages.
Copy 4 of 119 copies. Series A

Contract No. W-7405-eng-26

# NEUTRON FLUX AND TISSUE DOSE STUDIES WITH FISSION THRESHOLD DETECTORS

## PART I. EXPERIMENTAL MEASUREMENTS

G. S. Hurst
J. A. Harter
P. N. Hensley
W. A. Mills

## PART II. CALCULATION OF THE SPECTRUM IN AIR FROM A FISSION SOURCE

R. H. Ritchie

Date Issued

---

OAK RIDGE NATIONAL LABORATORY
Operated by
CARBIDE AND CARBON CHEMICALS COMPANY
A Division of Union Carbide and Carbon Corporation
Post Office Box P
Oak Ridge, Tennessee

[redacted]

MARTIN MARIETTA ENERGY SYSTEMS LIBRARIES
3 4456 0360656 9

## INTERNAL DISTRIBUTION

1. C. E. Center
2. Biology Library
3. Health Physics Library
4-5. Central Research Library
6. Reactor Experimental Engineering Library
7-26. Laboratory Records Department
27. Laboratory Records, ORNL R.C.
28. C. E. Larson
29. L. B. Emlet (K-25)
30. J. P. Murray (Y-12)
31. A. M. Weinberg
32. E. H. Taylor
33. E. D. Shipley
34. K. Z. Morgan
35. F. C. VonderLage
36. R. C. Briant
37. C. P. Keim
38. J. H. Frye, Jr.
39. R. S. Livingston
40. J. A. Swartout
41. S. C. Lind
42. F. L. Culler
43. A. H. Snell
44. A. Hollaender
45. M. T. Kelley
46. A. S. Householder
47. T. A. Lincoln
48. C. S. Harrill
49. C. E. Winters
50. D. W. Cardwell
51. J. A. Lane
52. E. E. Anderson
53. G. S. Hurst
54. J. A. Harter
55. R. H. Ritchie
56. P. N. Hensley
57. W. A. Mills
58. H. P. Yockey
59. E. P. Blizard
60. D. D. Cowen

## EXTERNAL DISTRIBUTION

61-62. Argonne National Laboratory
63-64. Armed Forces Special Weapons Project (Sandia)
65. Armed Forces Special Weapons Project, Washington
66-68. Atomic Energy Commission, Washington
69. Brookhaven National Laboratory
70-71. Carbide and Carbon Chemicals Company (K-25 Plant)
72-73. duPont Company, Augusta
74-75. General Electric Company (ANPP)
76-78. General Electric Company, Richland
79-80. Hanford Operations Office
81. Kirtland Air Force Base
82-83. Knolls Atomic Power Laboratory
84-85. Los Alamos Scientific Laboratory
86. Mound Laboratory
87. Naval Research Laboratory
88-89. New York Operations Office
90-91. Phillips Petroleum Company
92. Public Health Service
93. Sandia Corporation
94. San Francisco Operations Office
95. USAF Headquarters
96. U. S. Naval Radiological Defense Laboratory
97. UCLA Medical Research Laboratory (Warren)
98-99. University of California Radiation Laboratory, Berkeley
100-101. University of California Radiation Laboratory, Livermore
102. University of Rochester
103-104. Westinghouse Electric Corporation
105-119. Technical Information Service, Oak Ridge

[redacted]

# PART I. EXPERIMENTAL MEASUREMENTS

## INTRODUCTION

The Radiation Instruments Branch, Division of Biology and Medicine, U.S.A.E.C., requested that the Health Physics Division of Oak Ridge National Laboratory make neutron measurements in connection with the Nevada test series Upshot/Knothole, Spring 1953. These neutron measurements would help in defining the tissue dose (energy dissipated per gram of average wet tissue) at different distances from the explosion. Such measurements were made and complete results reported in Project 24.2 report to the Test Director. The purpose of this report is to give a description of the methods and apparatus developed for the measurements.

Most of the neutron detection at previous tests had been done by gold (thermal neutron detector) and sulfur (threshold at about 2.5 Mev), therefore little was known about the number of neutrons with energies between thermal and 2.5 Mev. Since fission spectrum neutrons are largely in this energy region, we considered it important to have a detector that would be sensitive to these neutrons. Even though the tissue dose (Fig. 1) increases with neutron energy, it was anticipated that it would be significant in the intermediate (thermal to 2.5 Mev) energy region. It is noted here that the tissue dose* curve in Fig. 1 is a first collision curve, that is, in case of fast neutrons the curve when multiplied by the spectrum of neutrons actually entering a gram of tissue would give the energy dissipated in that gram. In the case of thermal neutrons the meaning of a first collision calculation is not so clear, since approximately half of the first collision dose

---

* The dose is given in rep units corresponding to an absorbed dose of 93 ergs per gram of soft tissue.

[redacted]

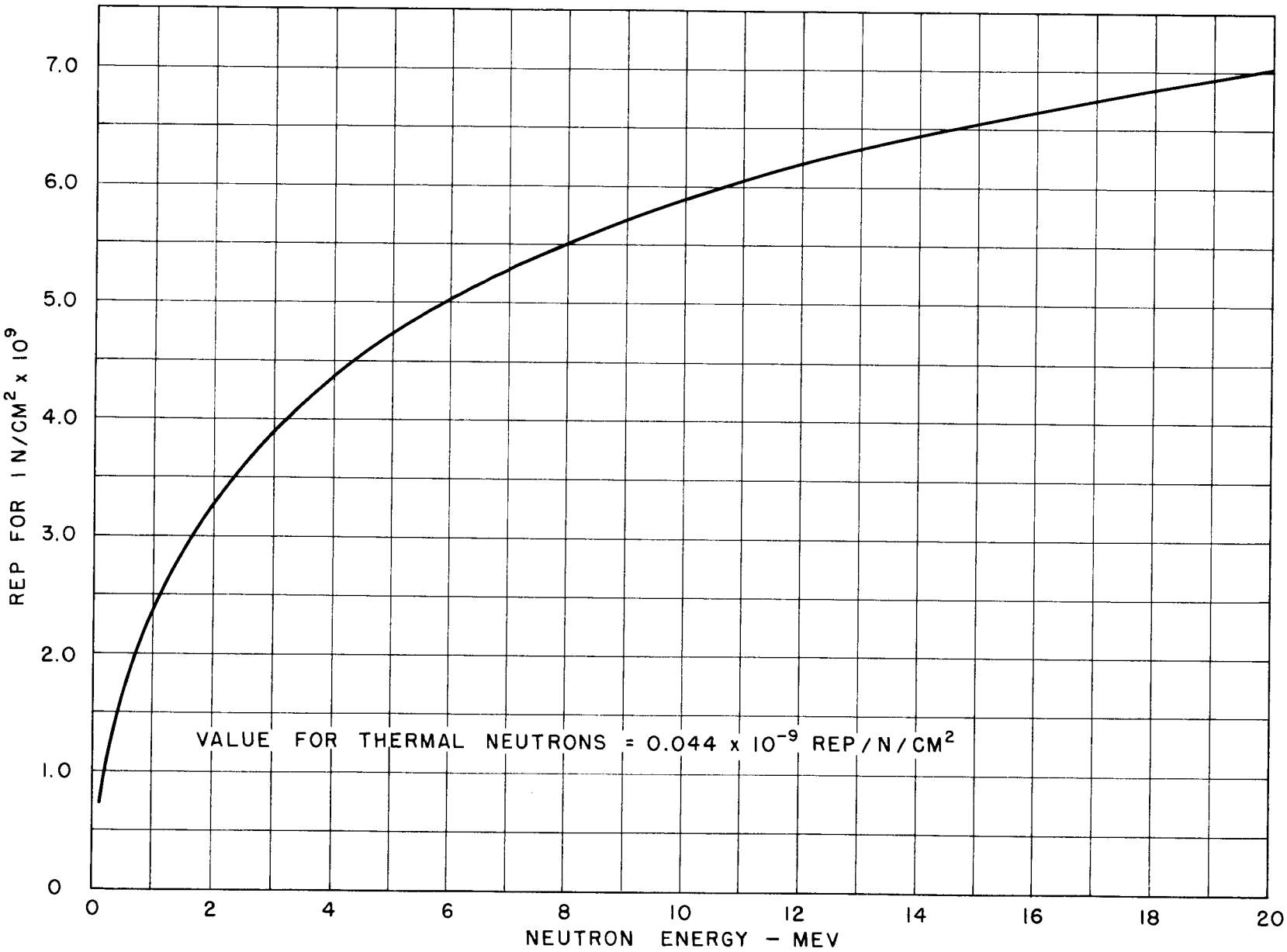


Fig. 1. First Collision Tissue Dose Curve, Using 1 rep = 95 ergs/gram Tissue.

would be due to the $H^1(n, \gamma)H^2$ reaction and the other half due to the $N^{14}(n, p)C^{14}$ reaction. Since protons are absorbed and not scattered out of the differential element where they are formed, the energy from the $N^{14}$ capture would be proportional to the thermal neutron flux entering the element. The energy contribution of the $H^1(n, \gamma)H^2$ reaction, to the differential element, would depend not only on the thermal neutron flux entering the element but would depend in part on the gamma scattering from neighboring elements. Perhaps the best way to determine the thermal neutron dose would be by measuring the thermal flux incident to a body and use the type of calculations used by Snyder[1] to determine the energy distribution for both reactions separately. In any case, for simplicity, we adopt a first collision dose for thermal neutrons and mean that the first collision dose is the energy that would be received per gram of a small element of tissue, not surrounded by other elements of tissue, but being large enough to bring the secondary electrons from the 2.1 Mev gamma ray into equilibrium.

Our objective now reduces itself to dividing the neutron spectrum into sufficient groups so that the curve in Fig. 1 can be used to determine the first collision tissue dose.

## ENERGY RESPONSE OF $Pu^{239}$, $Np^{237}$ AND $U^{238}$

In Fig. 2(a) we see that the fission cross section of $Pu^{239}$[2] is nearly constant from 0.03 Mev to 14.0 Mev. Thus, a measure of the number of fissions would indicate the total neutrons/$cm^2$ in this region. $Pu^{239}$ has a high thermal cross section (700 barns) which can be used to advantage in calibration of the number of fissions. During exposure to fast neutrons the thermal neutrons may be removed by $B^{10}$ shielding of the $Pu^{239}$. Shown also in Fig. 2(a) is the fission cross

1. Snyder, W. S., NUCLEONICS 6, No. 2, p. 46, February 1950.
2. Neutron Cross Sections, BNL-170.

section of $Np^{237}$[3] which has a threshold at approximately .4 Mev and is fairly flat above 1 Mev to 6 Mev. Another useful reaction is the fission of $U^{238}$[3] which is nearly constant from its threshold at 1.5 Mev to 6.0 Mev. Thus the use of these three fission detectors in conjunction with gold and sulfur permits the spectrum to be resolved into five energy groups.

If the fission cross section of $Pu^{239}$ is multiplied by the absorption factor $e^{-\sigma N}$ where $\sigma$ is the cross section of normal boron, and N is the number of boron atoms per $cm^2$, and if $N = 2.4 \times 10^{23}$ atoms/$cm^2$ the curve in Fig. 2(b) is obtained. A sphere 1-1/2" radius filled with $B_4C$ (70% boron) pulverized to give a density of 1.59 grams/$cm^3$ gives the equivalent absorption. The responses of the threshold detectors have been approximated by step-functions which are shown in Fig. 2(b). Also shown for comparison is the response of the $S(n, p)P^{32}$ reaction (from AECU-2040).

## SOURCES AND CONTAINERS

The Pu sources[4] consisted of 3/4" discs of solid metallic Pu, each containing approximately one gram of Pu. These were plated with Ni to reduce the alpha hazard. Uranium samples[5] were prepared in much the same manner. The one Np sample[6] (30 mg) that was available was prepared by deposition on a platinum disk. All samples were sealed in lucite containers which could be placed at the center of the boron container, Fig. 3.

## COUNTING SYSTEM

Since Pu emits several low energy gamma rays, the gammas from the fission products of Pu are counted with a NaI scintillation counter, the detector set so that it is sensitive to gamma rays with energy approximately greater than 0.9 Mev.

---

3. Supplement No. 1 to Neutron Cross Sections, BNL-170A.
4. We are indebted to Dr. Jane Hall, Los Alamos Scientific Laboratory, for the preparation of these sources.
5. Supplied by B. Harmatz, Oak Ridge National Laboratory.
6. Supplied and prepared by George Parker, Oak Ridge National Laboratory.

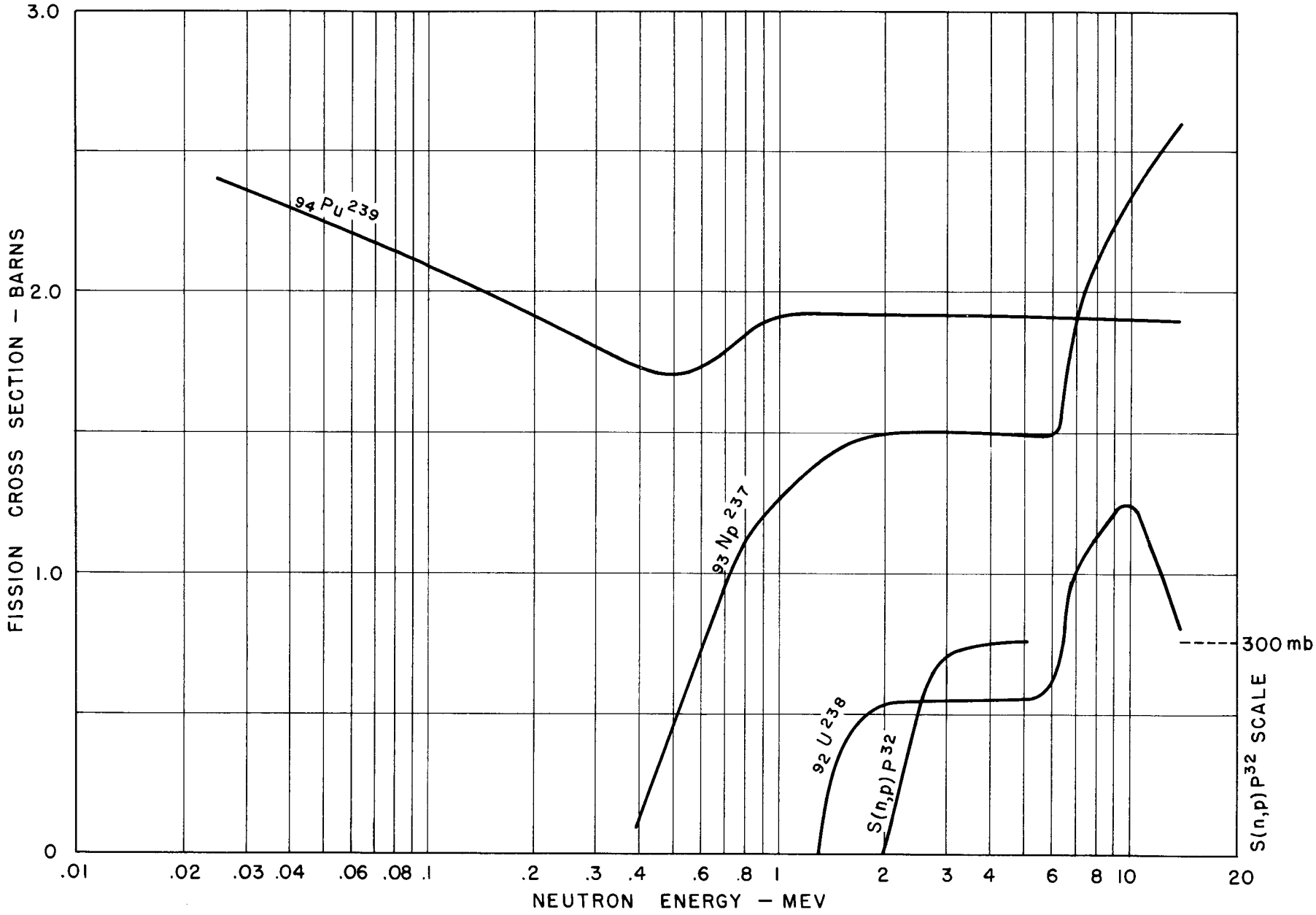


Fig. 2a. Fission Cross Sections of $Pu^{239}$, $Np^{237}$, and $U^{238}$.

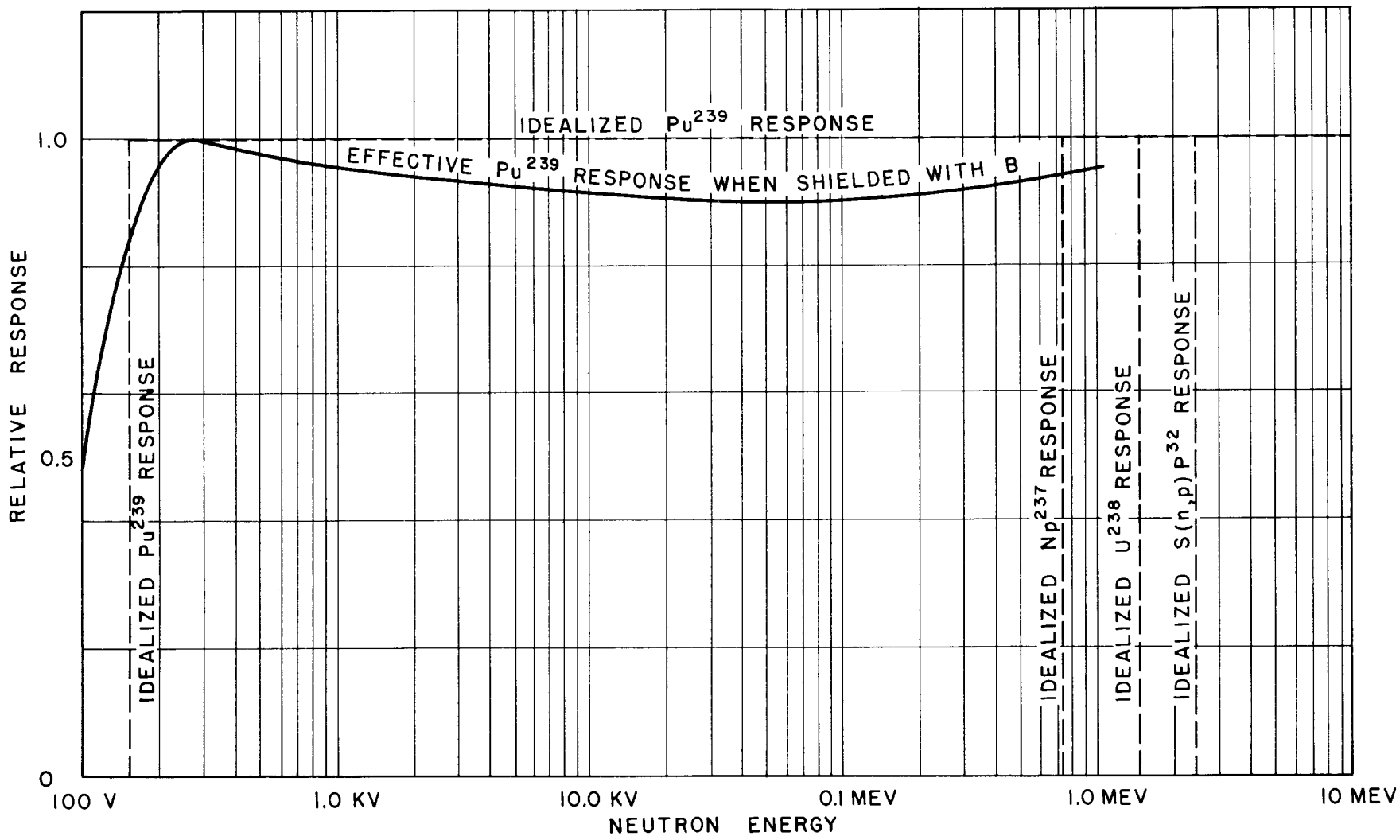


Fig. 2b. Response Curves and Step Function Approximations of the Threshold Detectors.

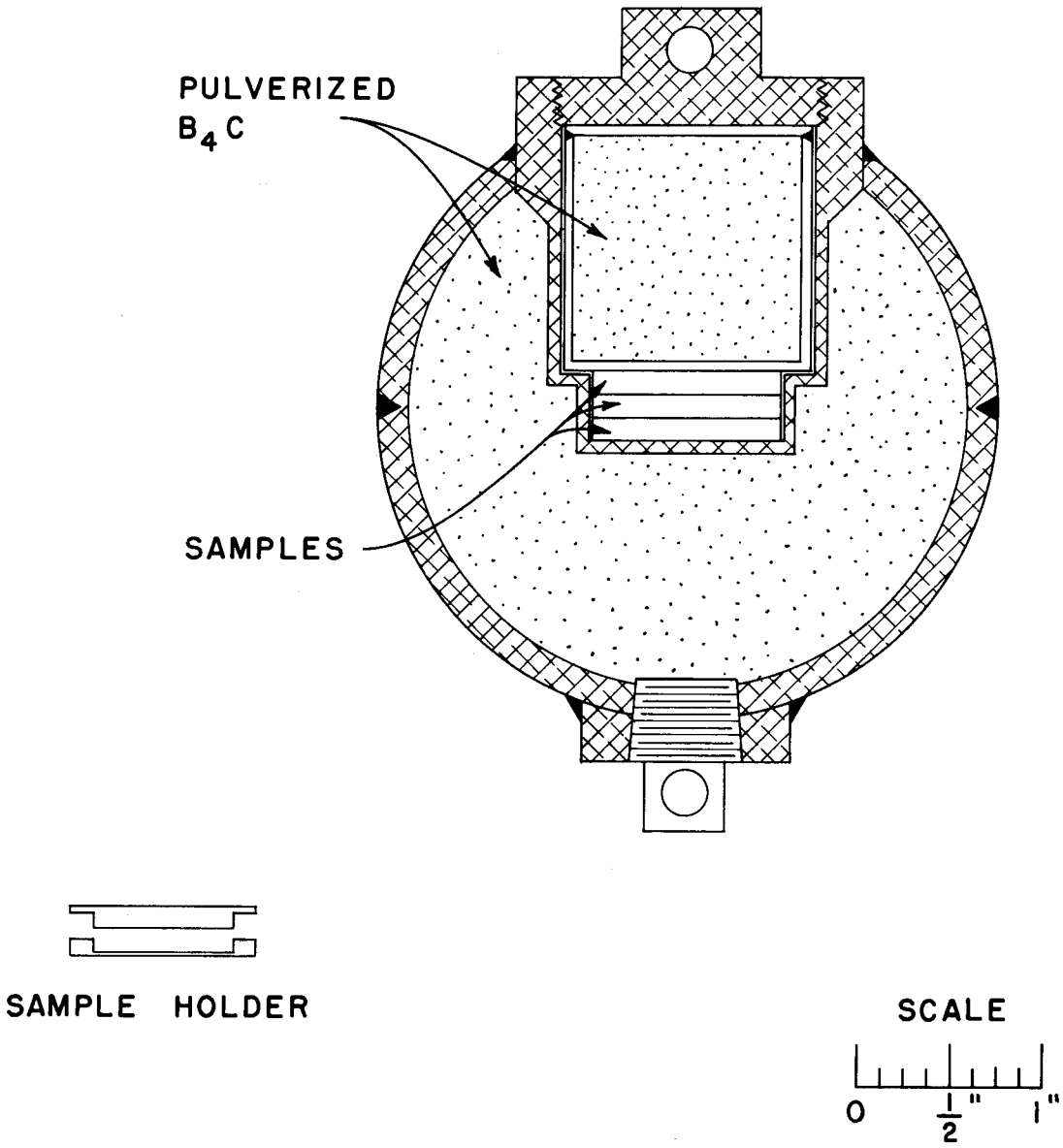


Fig. 3. Boron Container for Exposing Foils to Fast Neutrons.

A diagram of the NaI crystal, with lead shield to decrease the number of low energy gammas striking the crystal, is shown in Fig. 4. The entire assembly is shielded with two inches of lead (not shown in the diagram). The output of the photomultiplier is fed through a preamplifier to a linear amplifier and integral pulse height selector. With the bias energy at approximately 0.9 Mev the background with no source present is about 40 counts/min and the one gram Pu sample (before neutron irradiation) adds another 160 counts/min, making a total effective background of 200 counts/min.

## CALIBRATION OF COUNTER

As mentioned previously, the large fission cross section of $Pu^{239}$ in the thermal region makes the calibration of the entire system of threshold detectors very simple. The procedure is to irradiate a Pu sample for a short time to a known thermal flux. This sample is .1 gram and 3/4" in diameter; hence, thin enough so that the attenuation of these thermal neutrons incident normally is less than 5%. If a one gram foil (with boron shield to eliminate the thermal flux) is exposed to fast neutrons the ratio $\frac{\text{counts/n/cm}^2\text{ (thermal)}}{\text{counts/n/cm}^2\text{ (fast)}} = \frac{\sigma_{Th}}{\sigma_f} \times \frac{.1\text{ gm}}{1\text{ gm}} = \frac{700}{2} = \frac{1}{1} = 35.0$, holds at any given time after irradiation. The Pu curve shown in Fig. 5 was, thus, constructed by following the decay of the 0.1 gram Pu calibration sample. The Np and U curves are obtained from the Pu curve by correcting for the difference in cross section, i.e.,

$$\frac{\text{counts/n/cm}^2\text{ Pu}}{\text{counts/n/cm}^2\text{ Np}} = \frac{2.0}{1.5} = 1.33$$

and

$$\frac{\text{counts/n/cm}^2\text{ Pu}}{\text{counts/n/cm}^2\text{ U}} = \frac{2.0}{.43} = 4.65$$

at the same time after irradiation and for equal masses.

UNCLASSIFIED ORNL-LR-DWG. 361

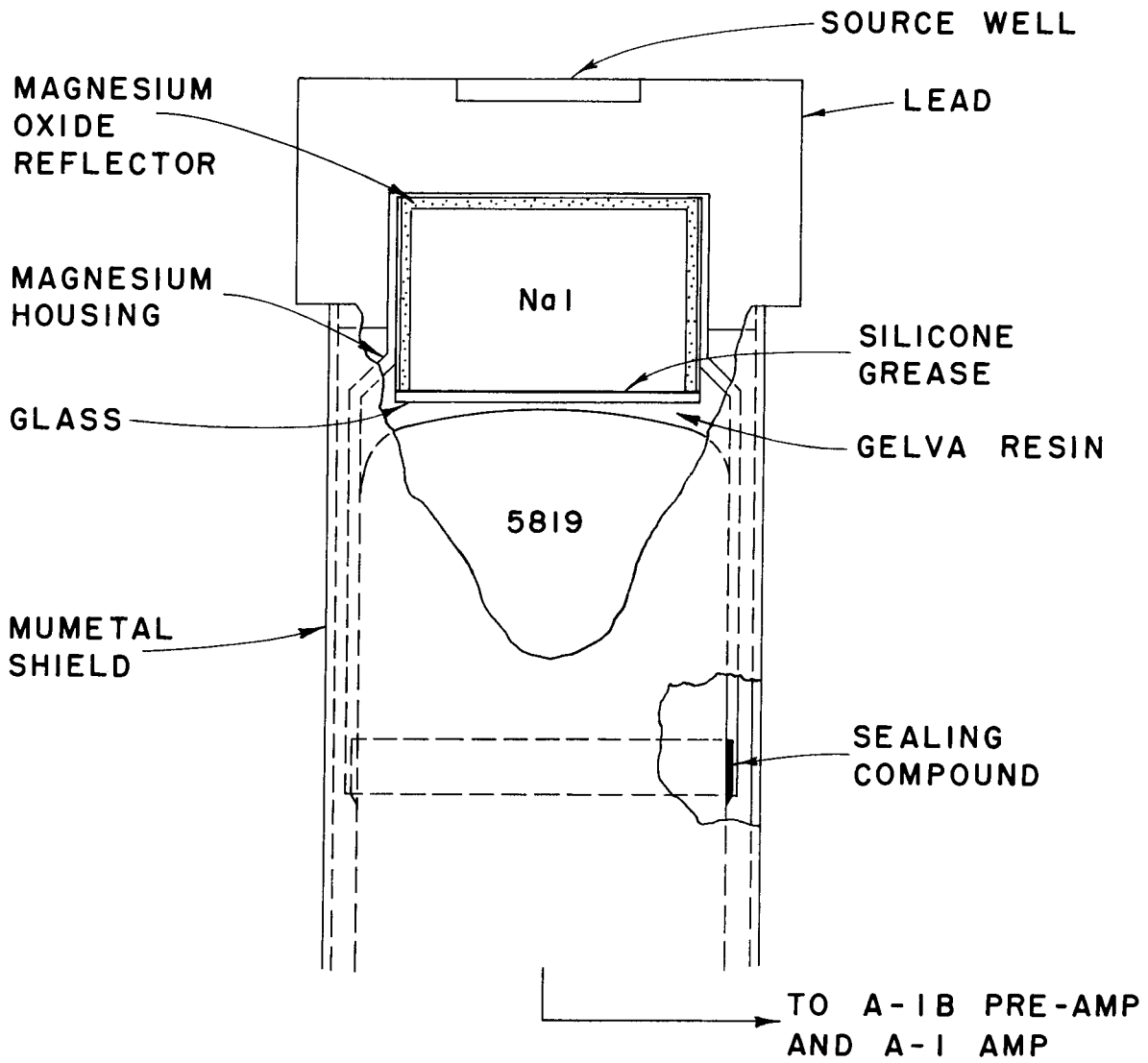


Fig. 4. Diagram of the Gamma-Ray Scintillation Detector.

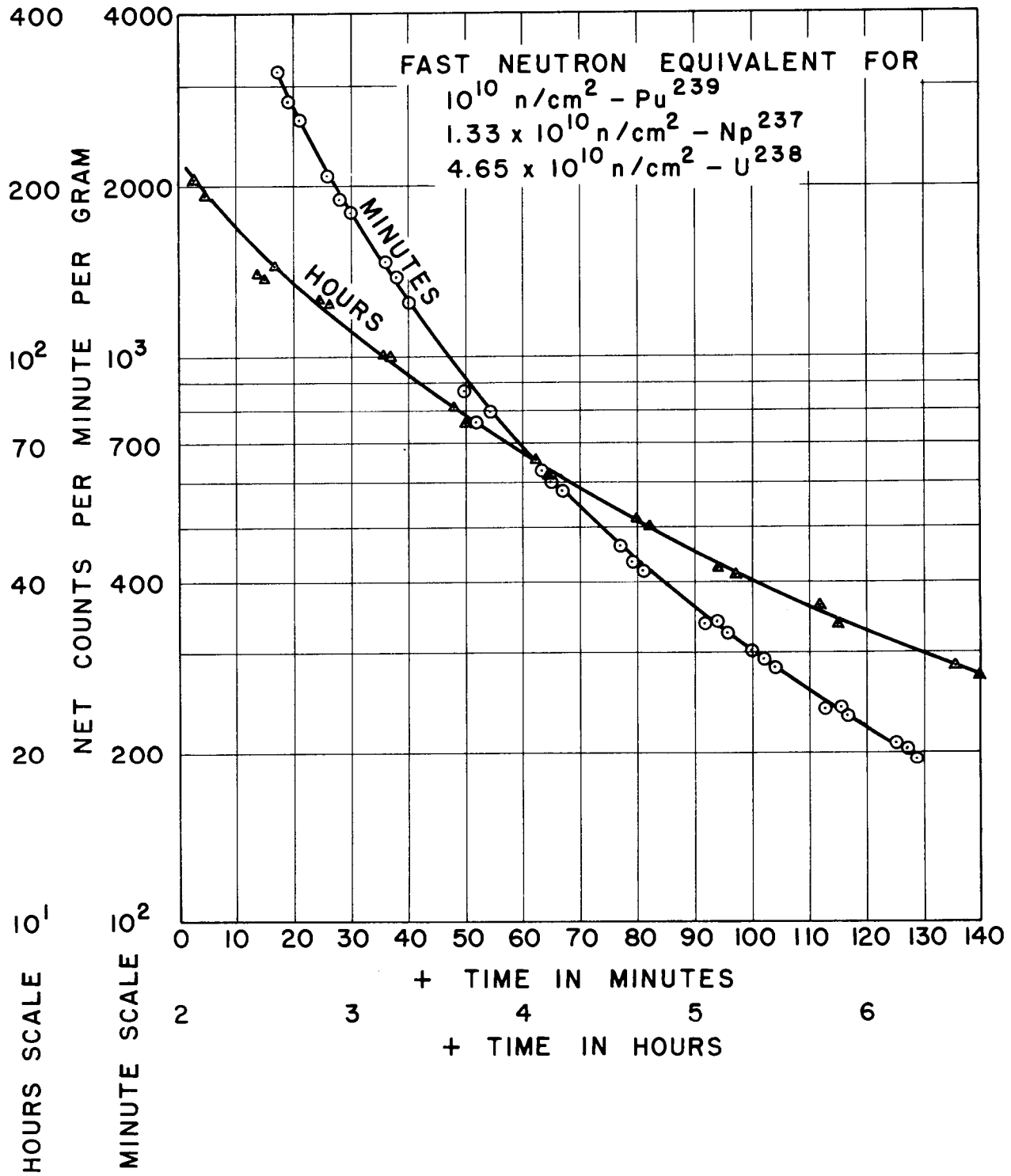


Fig. 5. Scintillation Count Rate vs Time for Indicated Fast Neutron Flux.

In the case of $Np^{237}$ there is one difficulty; namely, that the reaction $Np^{237} + {}_0n^1 \longrightarrow Np^{238}$ is competitive with the fission reaction. $Np^{238}$ has a 1.0 Mev gamma with a half-life of 2.1 days. One might eliminate this gamma by using a higher bias when counting Np. In any case the number of fission ($N_f$) can be determined from the counts vs. time ($N_t$) by obtaining the best fit to the equation

$$N_t = N_f \times C_t + N_a e^{-.693t/50}$$

where $C_t$ is the experimental count rate at time, t, for fission of Pu; $N_a$ is the count rate at time zero due to the thermal neutron activation, where t is given in hours.

A very important experimental detail is that the entire counting system must be standardized frequently, and this may be done by using a gamma source at a known distance above the detector. For example, if 0.25 millicuries $Co^{60}$ is placed at 40.0 cm above the lead shield on the NaI crystal, the count rate is 440 counts/64 in one minute with energy bias set at 0.9 Mev.

## TYPICAL FIELD RESULTS

Typical results obtained for one station and one shot are shown in Fig. 6. The histogram plot shows the number of neutrons in each energy interval, where it is noted that the predominate number is between the gold and sulfur thresholds. Rep figures in the second column, obtained by multiplying the number of neutrons in each interval by the curve in Fig. 1, for the mean energy of the interval, show that the major part of the tissue dose is detected by Pu, Np, and U.

## ACKNOWLEDGEMENT

The authors are grateful for the helpful suggestions of K. Z. Morgan, P. R. Bell, J. S. Cheka, J. B. Trice, and H. H. Hubbell. We wish also to thank Grace McCammon for the thermal neutron calibrations.

Dwg. 20424

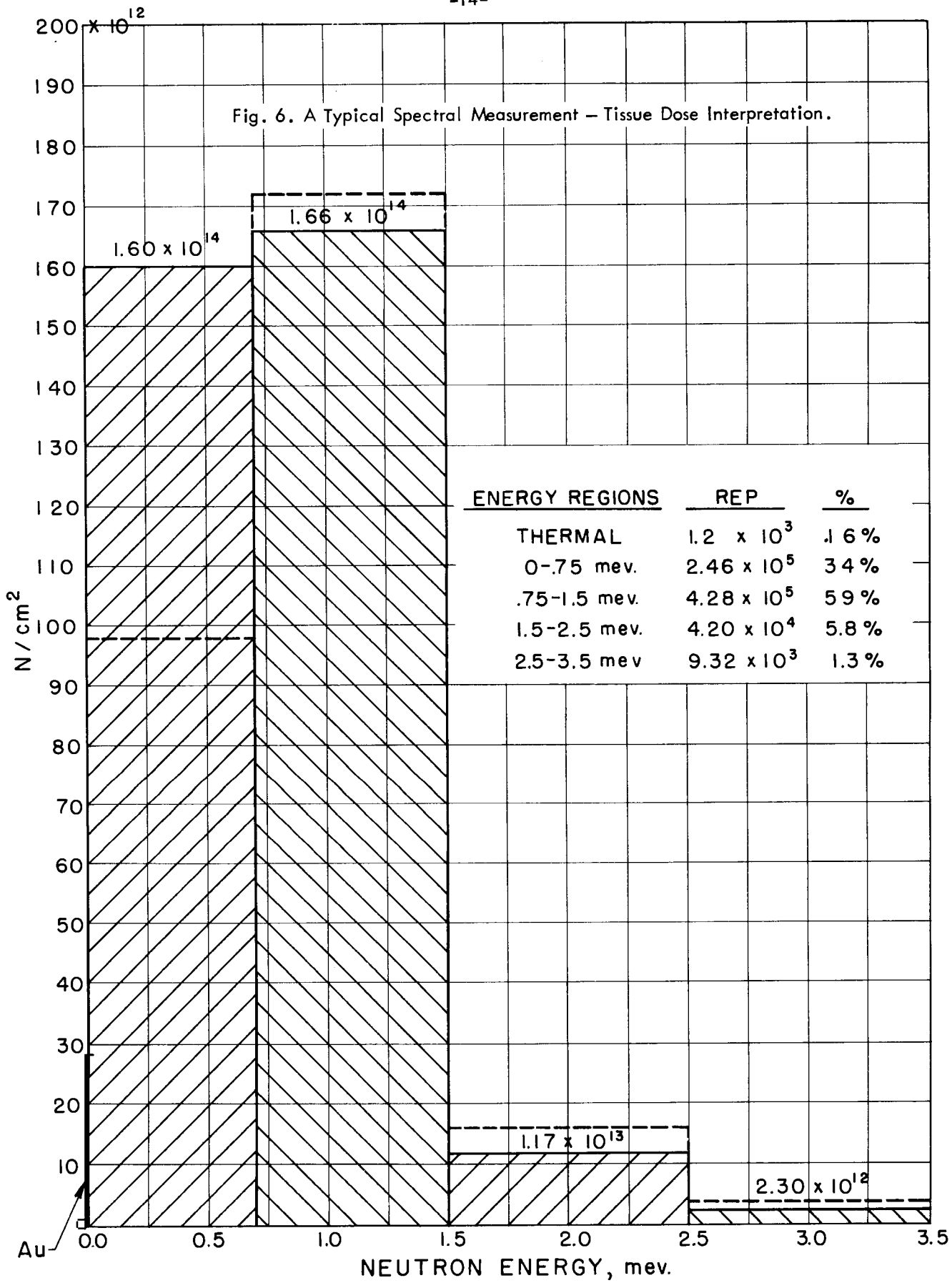


| ENERGY REGIONS | REP | % |
|---|---|---|
| THERMAL | $1.2 \times 10^3$ | .1 6 % |
| 0-.75 mev. | $2.46 \times 10^5$ | 34 % |
| .75-1.5 mev. | $4.28 \times 10^5$ | 59 % |
| 1.5-2.5 mev. | $4.20 \times 10^4$ | 5.8 % |
| 2.5-3.5 mev | $9.32 \times 10^3$ | 1.3 % |

Fig. 6. A Typical Spectral Measurement – Tissue Dose Interpretation.

# PART II. CALCULATION OF THE SPECTRUM IN AIR FROM A FISSION SOURCE

## INTRODUCTION

To supplement the measurements described in the first portion of this report an exploratory age theory calculation has been made of the neutron spectrum at Station 14 during shot Grable.

This series of measurements offers one of the first opportunities for comparison of experiment and theory on the spectral degradation of fast neutrons. For this reason it was felt that such a comparison is important even though there is some uncertainty concerning the abundance and cross sections of the various nuclei involved.

The conditions existing during the measurement on shot Grable seem to be good for the application of age theory if capture and inelastic processes may be neglected. It is understood that there was no tamper material included in this shot so that one may consider the source spectrum as known, although structures around the fissionable material may affect the spectrum somewhat. The measurements were made far enough from the center of the explosion that many collisions with air nuclei are made by an "average" neutron reaching the threshold detector. On the other hand, the distance is small enough so that the criteria for application of age theory are fulfilled.

## AGE THEORY SOLUTION

The solution of the idealized problem of a point source in an infinite homogeneous medium has a simple solution in the age theory of Fermi[7] when (1) scattering is nearly isotropic in the laboratory system of coordinates, (2) when the scattering cross sections do not vary rapidly with energy, (3) when

---

7. Marshak, R. E., Rev. Mod. Phys. 19, 212 (1947).

absorption is small, and (4) when the average number of slowing down collisions is large. The age approximation breaks down at distances of the order of the age divided by the mean free path. For larger distances the approximate age-first collision procedure[8] may be used. In this case one must employ the function tabulated by Rosser[9].

For a point source of neutrons of unit strength (one neutron/sec) which is monokinetic at the energy $E_o$, the age theory solution with zero capture is[8]

$$\psi_{01}(r, u_o, u) = \frac{1}{\xi \Sigma_s(u)} \frac{e^{-r^2/4\tau(u,u_o)}}{[4\pi\tau(u,u_o)]^{3/2}} \tag{1}$$

where $\psi_{01}(r, u_o, u)\, du$ is the flux of neutrons (neutrons/cm$^2$ sec) at a distance r from the source with energies in the interval du at u. The logarithmic energy variable $u = \ln \frac{10}{E(\text{Mev})}$ has been employed here. The definitions of the other symbols are given in the appendix.

For the two medium problems with no capture the solution is[10]

$$\psi_{02} = \frac{1}{\xi \Sigma_s(u)} \left\{ \frac{E_1[r^2/4\tau(u,u_o)] - E_1[\rho^2 r^2/4\tau(u,u_o)]}{[1 - 1/\rho^2][4\pi\tau(u,u_o)]^{3/2}} \right\} \tag{2}$$

---

8. Weinberg, A. M. and L. C. Noderer, AECD-3471, p. III-39.

9. Rosser, J. B., Theory and Application of $\int_0^x e^{-x^2} dx$ and $\int_0^z e^{-p^2 y^2} dy \int_0^x e^{-x^2} dx$, Mapleton House (1948).

10. Bellman, R., R. E. Marshak and G. M. Wing, Phil. Mag. 40, 297 (1949).

where $\rho$ is the ratio of ground density to air density. This solution assumes that both ground and air nuclei have similar scattering properties. Although this is not strictly true the formula should be approximately valid in the limit of very large $\rho$. The Eq. (2) gives the flux at the detector when source and detector are separated a distance r and are both located on the boundary between the two media. The function

$$E_1(x) = \int_x^\infty e^{-u}\, du/u \tag{3}$$

When capture is present the solution $\psi_{01}$ in the infinite homogeneous medium is merely multiplied by the quantity

$$\exp\left\{ - \int_{u_0}^{u} \frac{\Sigma_a(u)}{\xi\, \Sigma_s(u)}\, du \right\} \tag{4}$$

The two medium problem with capture in age theory is not expressible in closed form.

If the source has a distribution of energies $N(u_0)du$ in the interval $du_0$ at $u_0$, then the resultant total flux in du at u is

$$\psi_{1,2}(r,u) = \int_0^u du_0\, N(u_0)\, \psi_{01,02}(r, u_0, u) \tag{5}$$

where it is tacitly assumed that the source spectrum has no energies greater than 10 Mev.

It is known that elastic shadow scattering of fast neutrons on nuclei is of consequence at high energies[11]. In this event scatter becomes anisotropic in the center of mass system. The age theory framework may be generalized to include

11. NYO-636, Final Report of the Fast Neutron Data Project.

this case by a straight forward procedure and the results are given in Appendix II. However, the available evidence seems to indicate that in the energy range in which the bulk of fission neutrons lie scatter on air nuclei is still nearly isotropic in the center of mass system. Consequently shadow scatter was neglected in this calculation.

## CALCULATIONS

1. Cross Sections. Scattering and absorption cross sections of nitrogen and oxygen were taken from AECU-2040. It was assumed that scatter on N and O is isotropic in the center of mass system. The composition of the air was taken to be 79% $N_2$ and 21% $O_2$ at a density of 0.0011 gm/cm$^3$ corresponding to an elevation of 3080 ft, which is the elevation of the playa in Frenchman Flat[12]. The age $\tau(u)$ is plotted in Fig. 7 as a function of the "lethargy", $u = \ln \frac{10}{E(\text{Mev})}$, which was chosen for convenience in calculation.

2. Source Spectrum. In Fig. 8 is given a plot of the empirical equation for the fission spectrum[13];

$$N(u)\,du = 10\sqrt{\frac{2}{\pi e}}\,\sinh\left(\sqrt{20}\,e^{-u/2}\right)\exp\left(-10e^{-u} - u\right)du$$

where e is the base of natural logarithms.

3. Source-Detector Separation. This was 1580 ft for the exposures made during shot Grable.

## RESULTS

In Fig. 9 are plotted the experimental histogram and spectra calculated by numerical integration of Eq. (5). The fission distribution is also plotted in

---

12. WT-518.
13. Watt, B. E., Phys. Rev. 87, 1037 (1952); Nereson, N., Phys. Rev. 88, 823 (1952).

UNCLASSIFIED
ORNL-LR-DWG. 358

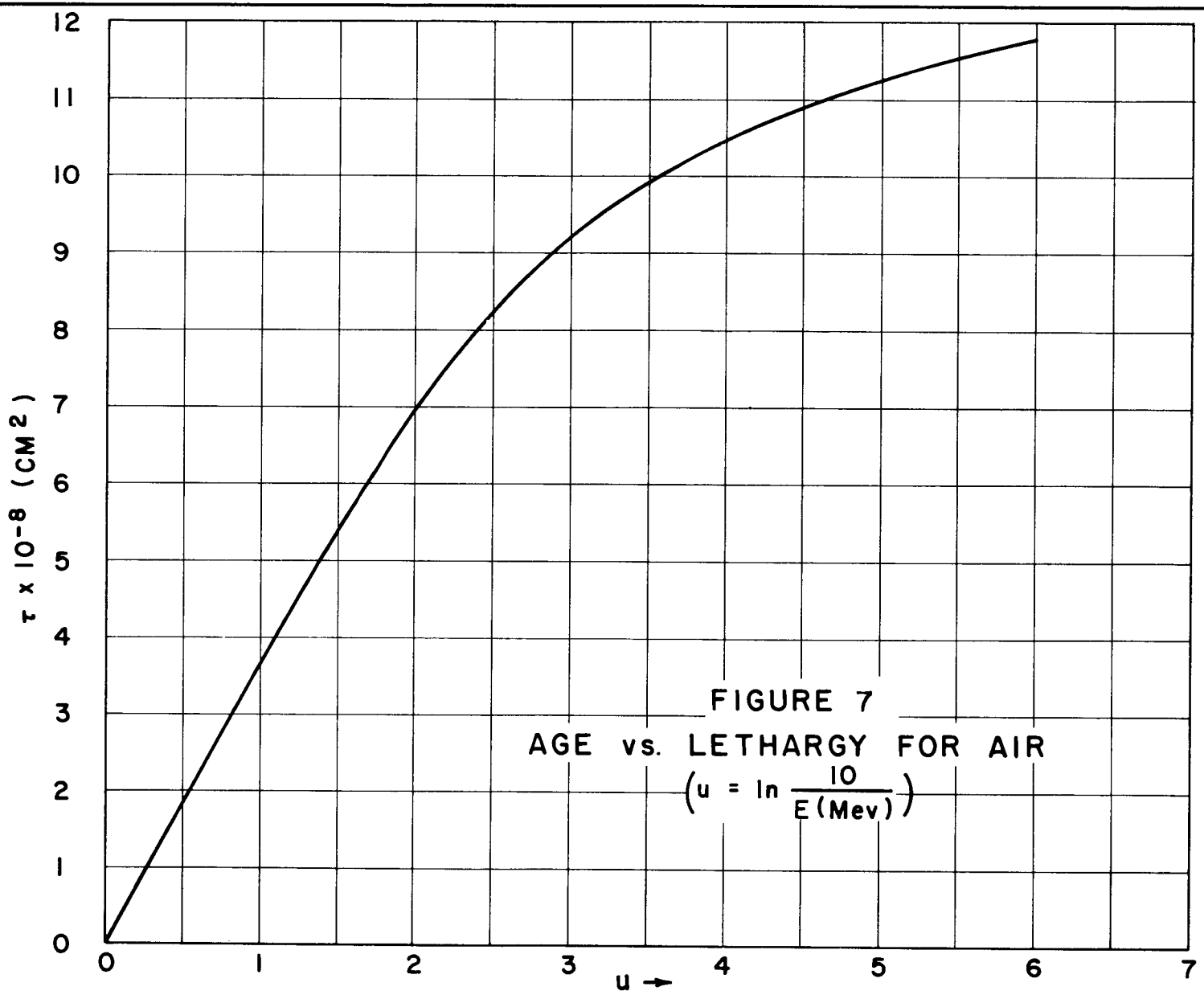


FIGURE 7
AGE vs. LETHARGY FOR AIR
$\left(u = \ln \frac{10}{E(\text{Mev})}\right)$

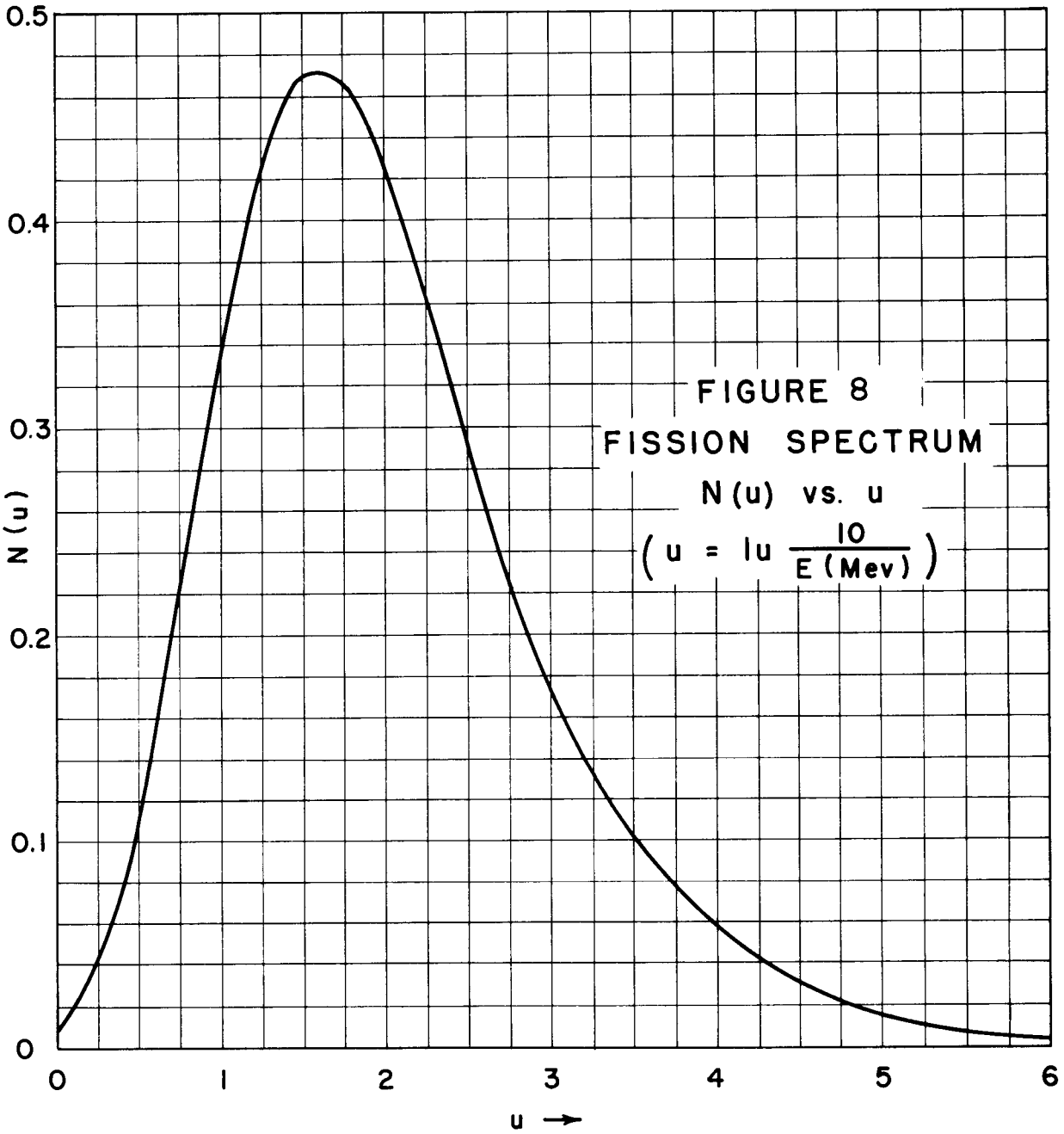


FIGURE 8
FISSION SPECTRUM
N(u) vs. u
$\left( u = \ln \frac{10}{E\,(\text{Mev})} \right)$

UNCLASSIFIED
ORNL-LR-DWG. 360

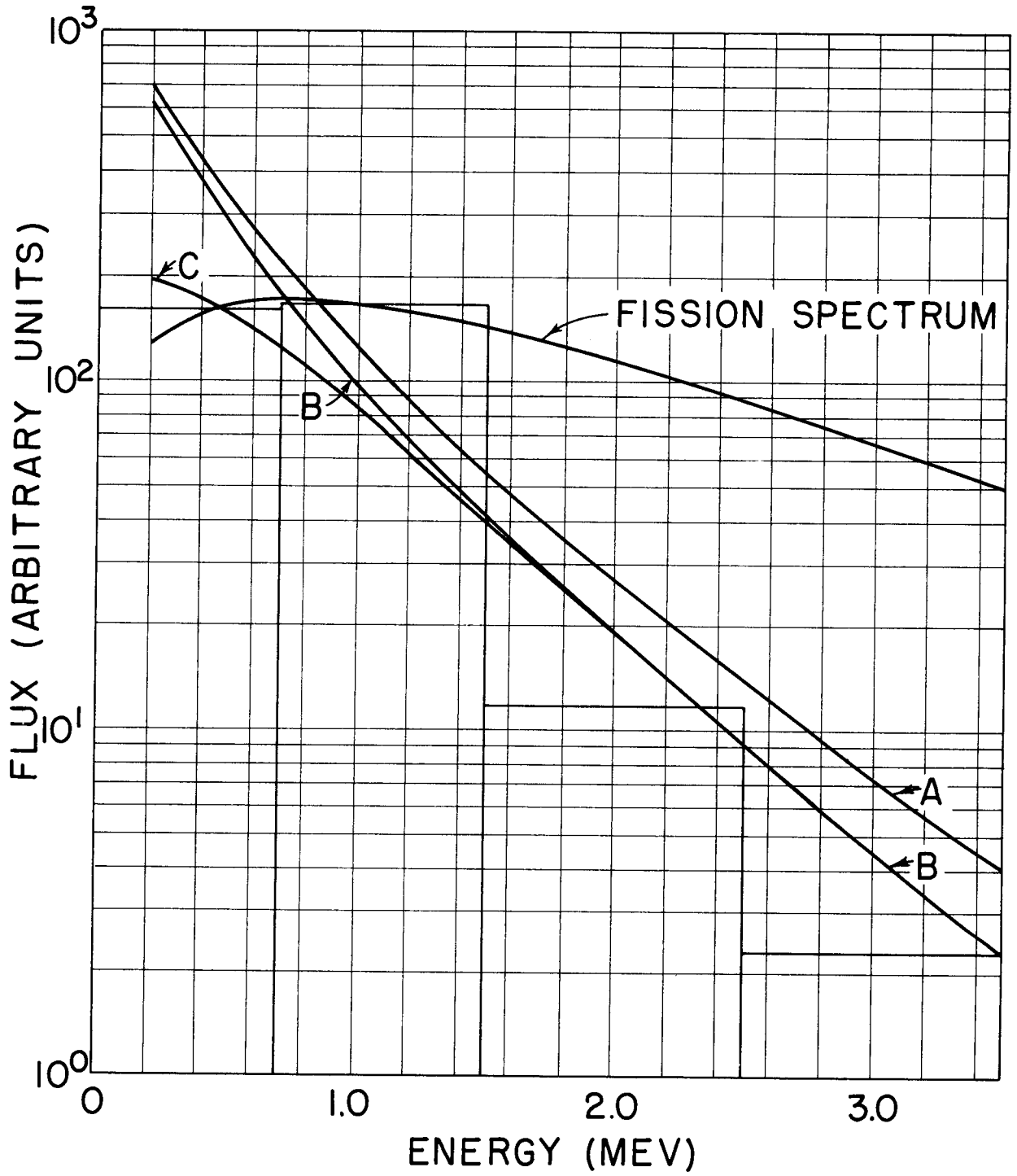


FIGURE 9

COMPARISON OF CALCULATED AND EXPERIMENTAL SPECTRUM

this figure. Since there was no information available on the absolute strength of the source, the calculated curves have been arbitrarily normalized for purposes of comparison.

It is seen that slowing down of neutrons in air and ground is indeed important since there is clearly a great deal of difference in the source spectrum and the experimental curves. Curve A was calculated from age theory assuming an infinite medium of air while curve B was calculated from the two medium solution. The slope of the experimental curve is reproduced reasonably well at the high energy end with better agreement for the two medium solution. Both curves, A and B, are too high in the low energy region which is probably due to neglect of absorption and inelastic scatter. In addition the presence of hydrogen in the soil is probably felt in this region.

To obtain a rough estimate of this effect it was assumed that the ground is 5% by weight of $H_2O$ (in the form of, e.g., $3SiO_2 \cdot H_2O$) and that half of the collisions with hydrogen are equivalent to absorption. The absorption multiplier, Eq. (4), was computed on this basis and used as an empirical correction to the two medium solution. The resulting spectrum is given in curve C.

A more exact calculation should probably include the effect of absorption on heavy elements and hydrogen scatter in the ground. It would be desirable to compare the absolute values of the calculated flux with the experimental values if information on the source strength can be obtained. Experimental data on the spectrum at other distances from the shot would be very desirable so that a more thorough comparison can be made.

ACKNOWLEDGEMENT

The writer would like to express his thanks to H. P. Yockey and G. S. Hurst for their helpful comments and criticisms.

## APPENDIX I

### Meaning of Symbols

$$\overline{\xi \Sigma_s(u)} = \sum_i N_i \xi_i \sigma_{si}(u)$$

$$\Sigma_t = \sum_i N_i \sigma_{si}(u)(1 - \overline{\cos\theta_i})$$

$$\Sigma_a = \sum_i N_i \sigma_{ai}(u)$$

$$\tau(u,u_0) = \int_{u_0}^{u} du / 3\Sigma_t \overline{(\xi \Sigma_s)}$$

$\tau(u,u_0)$ = symbolic age of neutron with energy E originating at $E_0$.

$\xi_i$ = average logarithmic energy loss in collision with $i^{th}$ kind of nucleus.

$N_i$ = number per unit volume of $i^{th}$ kind of nucleus present in the scattering medium.

$\sigma_{si}$ = scattering cross section of $i^{th}$ nucleus.

$\sigma_{ai}$ = absorption cross section of $i^{th}$ nucleus.

$\overline{(\cos\theta)}_i$ = average cosine of deflection angle in the laboratory system in scatter on $i^{th}$ nucleus.

## APPENDIX II

### Generalization of Age Theory to Include Forward Elastic Scatter

Beginning with the stationary one-dimensional non-capturing form of the Boltzmam equation (in Marshak's notation[7]) one writes

$$\ell(u)\mu \frac{\partial \Psi}{\partial z} + \Psi(z,\mu,u) = \int_0^u du' \int d\hat{\Omega}\, \Psi(z,\mu',u')\, f(\mu_0, u' \to u)$$

where $\Psi$ is the collision density in phase space, $f(\mu_0, u' \to u)$ is the relative probability that a neutron of lethargy u' will be scattered through an angle $\cos^{-1}\mu_0$ into the lethargy interval du at u. The quantity $f(\mu_0, u' \longrightarrow u)$ may be expressed as

$$f(\mu_0, u' \to u) = g(\mu_0, u')\, \delta\left[\mu_0 - \left(\frac{M+1}{2} e^{-(u-u')/2} - \frac{M-1}{2} e^{+(u-u')/2}\right)\right]$$

which exhibits the connection between energy loss and scatter angle. $g(\mu_0, u')$ is the relative probability that a neutron of lethargy u' shall undergo scatter through the angle $\cos^{-1}\mu_0$.

Expanding $\Psi(z, \mu, u)$ in spherical harmonics, using the addition theorem for spherical harmonics and expanding the lethargy dependence of the Legendre moments in a Taylor series, one finds,

$$-\frac{\ell^2(u)}{3\left[1-\langle\mu_0(u)\rangle\right]} \frac{\partial^2}{\partial z^2} \Psi_0 = \left[G(u)-1\right]\Psi_0 - \xi(u) \frac{\partial \Psi_0}{\partial u} + \text{source term}$$

where

$$G(u) = \int_{u-\xi_M}^{u} du' \int d\hat{\Omega}_0\, f(\mu_0, u' \to u)$$

[redacted]

$$\langle \mu_0(u) \rangle = \int_{u-q_M}^{u} du' \int \mu_0 \, d\hat{\Omega}_0 \, f(\mu_0, u' \to u)$$

$$\xi(u) = \int_{u-q_M}^{u} du' (u-u') \int d\hat{\Omega}_0 \, f(\mu_0, u' \to u)$$

$$\Psi_0(z,u) = \int d\hat{\Omega} \, \Psi(z,\mu,u)$$

Letting the generalized age $\tau$ be

$$\tau(u) = \int_0^u \frac{\ell^2(u) \, du}{3\xi(u)\left[1 - \langle \mu_0(u) \rangle\right]}$$

and generalizing to three dimensional space, one finds for the flux

$$\psi_0(\bar{r},u) = \frac{1}{\xi(u) Z_s(u)} \, e^{-\int_0^u \frac{[G(u)-1]}{\xi(u)}} \, \chi(\tau[u], \bar{r})$$

where $\chi(\tau, \bar{r})$ satisfies

$$\nabla^2 \chi = \frac{\partial \chi}{\partial \tau} \quad \text{- source term.}$$

[redacted]